Spin transport in semiconductor quantum devices

Student: Ben Thorpe
Supervisors: Sophie Schirmer, Karol Kalna and Frank Langbein
College of Science (Physics), Swansea University, Singleton Park, Swansea, SA2 8PP, United Kingdom

ENGINEERING RESEARCH NETWORK WALES
RHWYDWAITH YMCHWIL PEIRIANNEG CYMRU
Noddir gan Lywodraeth Cymru
Sponsored by Welsh Government
Cyngor Cyllido Addysg Uwch Cymru
Higher Education Funding Council for Wales
hefcw

Abstract

We augmented an ensemble Monte-Carlo semiconductor device simulator [3] to incorporate electron spin degrees of freedom using a Bloch equation model to investigate the feasibility of spintronic devices. Results are presented for the steady state polarization and polarization decay due to scattering and spin orbit coupling for a III-V MOSFET device as a function of gate voltages, injection polarization and strain.

1. Theory

Following [4] we augmented a conventional Monte Carlo simulation of a InAlAs/InGaAs HEMT to incorporate electron spin.

Spin states described by the spin density matrix $\rho_0(t)$ given by $\rho_0(t) = \begin{pmatrix} \rho_{\uparrow\uparrow}(t) & \rho_{\uparrow\downarrow}(t) \\ \rho_{\downarrow\uparrow}(t) & \rho_{\downarrow\downarrow}(t) \end{pmatrix}$

Where $\rho_{\uparrow\uparrow}$ and $\rho_{\downarrow\downarrow}$ are the probabilities of finding an electron in a spin up or spin down state and the diagonal elements $\rho_{\uparrow\downarrow}$ and $\rho_{\downarrow\uparrow}$ represent the coherence.

ρ can be parametrised by a spin polarisation vector $\vec{S}_r = (s_x, s_y, s_z) = Tr(\sigma_r \rho(t))$ where $r = x, y, z$ and σ_r represents the Pauli matrices.

Spin polarisation vector of the current $\vec{S}_r = \langle \vec{S}_r(r,t) \rangle$ was obtained by averaging the components of the spin polarisation vectors of all electrons in a thin slice through the device channel located at position $x = R$ at time t.

The magnitude $|\vec{S}(R,t)| \leq 1$ defines the amount of polarisation, with 1 being defined as 100% spin polarisation in the direction of $\vec{S}(R,t)$.

Spin-orbit Coupling. Dyakonov-Perel-type spin dephasing was modelled using interaction Hamiltonians. For a structure grown in the [0,0,1] direction, where x is the transport direction along the channel, z is the growth direction orthogonal to the quantum well and α_{br} and Γ are material dependant constants:

- **Dresselhaus**: spin coupling to an electric field due to bulk asymmetry in the crystal

$$H_D = \Gamma \langle k_y^2 \rangle (k_z \sigma_y - k_x \sigma_x) \tag{1}$$

- **Rashba**: asymmetry in the potential due to the presence of a quantum well

$$H_R = \alpha_{br} (k_z \sigma_x - k_x \sigma_z) \tag{2}$$

Evolution of spin polarization vector. Rotation determined by the direction of the electron momentum

$$\rho(t+\tau) = e^{-i(H_R+H_D)\tau/\hbar} \rho(t) e^{i(H_R+H_D)\tau/\hbar}. \tag{3}$$

This exponential operator can then be written as a 2×2 scattering matrices

$$e^{-i(H_R+H_D)\tau/\hbar} = \begin{pmatrix} \cos(|\alpha|\tau) & i\frac{\alpha}{|\alpha|}\sin(|\alpha|\tau) \\ i\frac{\alpha^*}{|\alpha|}\sin(|\alpha|\tau) & \cos(|\alpha|\tau) \end{pmatrix} \tag{4}$$

where: $\alpha = \hbar^{-1}[(\eta k_z - \beta \langle k_y \rangle k_x) + i(\eta k_x - \beta \langle k_y \rangle k_z)]$

Our model neglects spin flips due to impurity or phonon scattering, the Elliott-Yafet mechanism, and spin relaxation caused by hyperfine coupling, based on the observation that Dyakonov-Perel mechanism is the dominant source of spin relaxation in Ga As[2] although such effects could easily be incorporated into the simulator.

2. Method

The spin-augmented device simulator was used to simulate spin transport in an $In_{0.3}Ga_{0.7}As$ MOSFET similar to those used in [3] (see Figs 1(a) and 1(b)). The spin orbit coupling constants $\beta = 2.681eVnm^3$ and $\eta = 0.768eVnm$ for the unstrained case were obtained from the $\vec{k} \cdot \vec{p}$ calculations detailed in Section 4.

The electrons were initially randomly polarised with the Bloch vectors evenly distributed across a sphere in real space such that there was initially no net magnetisation in the device. We then injected x, y and z polarised spins at the source and measured the average temporal and spatial distributions of the components of the Bloch vector across the device. This was done at a temperature of 300K for gate voltages varying between threshold and saturation for each device.

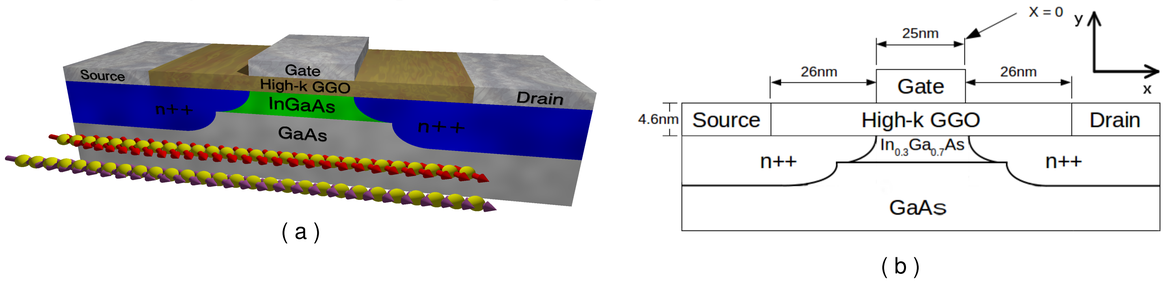

Figure 1: *(a) 3D model of $In_{0.3}Ga_{0.7}As$ MOSFET device showing spin polarisation of electrons along n-channel with 4% strain in the $[001]$ direction (Red) and unstrained (Purple). (b) Cross section of the 25-nm gate length, n-channel $In_{0.3}Ga_{0.7}As$ MOSFET*

3. Spin Transport Simulation Results

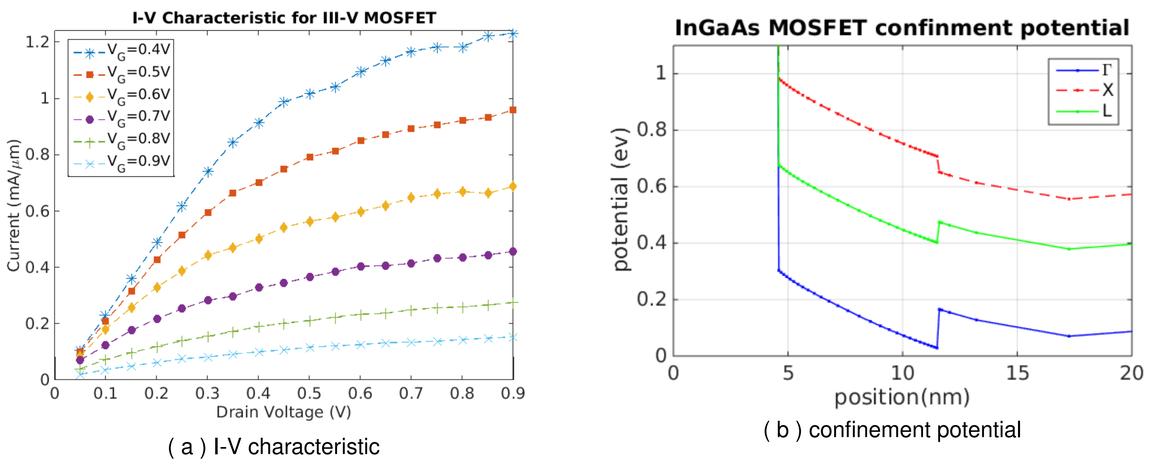

Figure 2: *Plots of the I-V characteristic and confinement potential obtained from the III-V MOSFET simulation.*

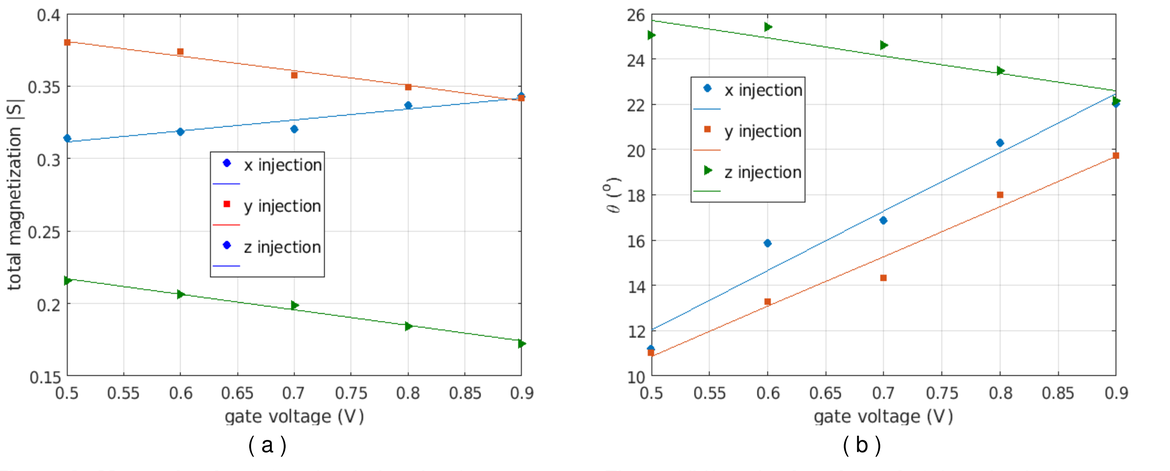

Figure 3: ***Magnetisation*** *$|S|$ at the drain edge ($x = 26nm$ see Figure 1(b)) and* ***azimuth angle*** *θ (rotation in the x-y plane) as a function of* ***gate voltage****.*

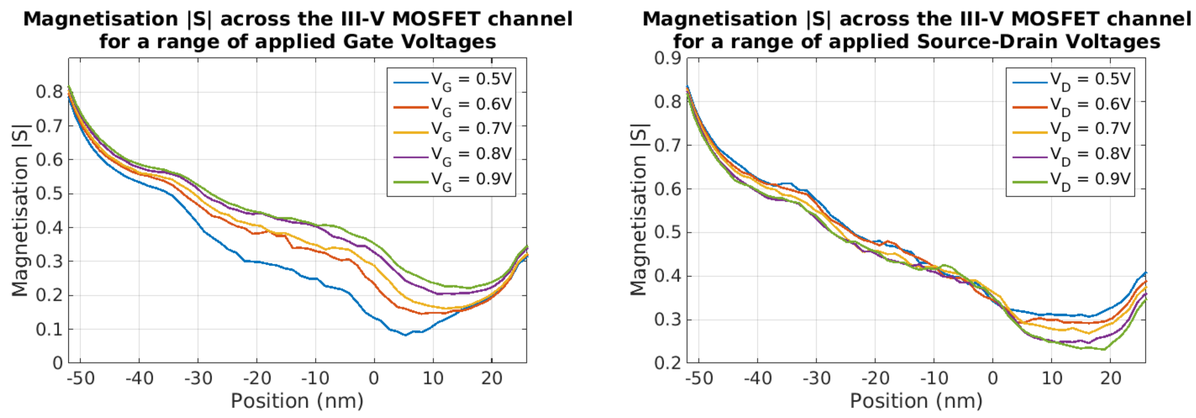

Figure 4: *Magnetization vs position along the channel for varying Gate and Source-Drain voltages for x-polarised spin injection taken at $t = 8ps$, i.e. after a steady state was reached.*

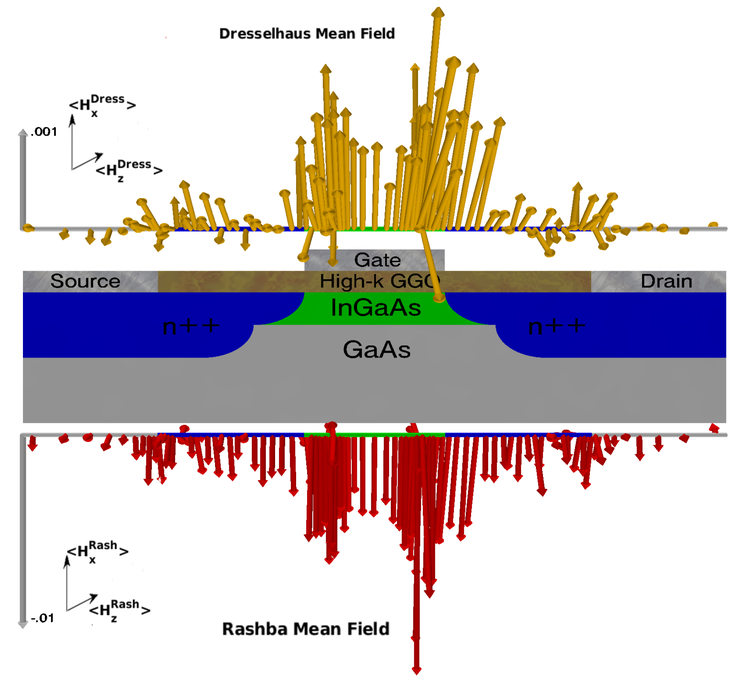

Figure 5: *Rashba and Dresselhaus mean field vectors H_R and H_D , obtained by averaging over all particles in thin slices across the channel for a single Monte Carlo run ($V_G = 0.9V$, $V_D = 0.5V$). The z-axis is in plane perpendicular to the channel but for the vector plots the axes have been rotated so that H_z is in the vertical direction for visual clarity.*

4. Strain effects

The effects of mechanical strain on the spin were investigated by means of $\vec{k} \cdot \vec{p}$ band-structure calculations.

$\vec{k} \cdot \vec{p}$ method: Efficient and accurate method for calculating band structures of many different semiconductor materials for both bulk and heterostructures.

This method involves using Lodwin perturbation theory to solve the Schrdinger equation about a point of high symmetry for a finite number of bands, accounting for the contribution from band interactions using physical parameters called Kane parameters and far band contributions with Luttinger parameters obtained from experimental data.

Adaptation for strain: Following Bir, Pirkus and Bahder [1]. An extra term is added to each element of the unstrained Hamiltonian created by replacing $k_x k_y$ (and it's circular permutations) with the component of the strain tensor ϵ_{xy} and the Luttinger parameters with deformation potentials.

Spin-Orbit Coupling: After calculating the band energies as a function of applied strain, The Dresselhaus and Rashba constants can be approximated using the inter-band energies at the Γ point along with 3 Kane parameters [2].

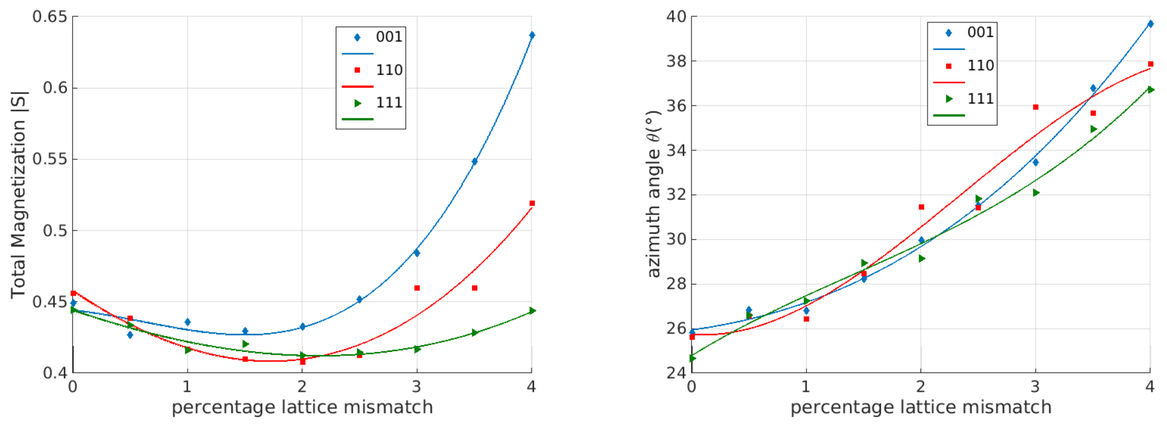

Figure 6: ***Magnetisation*** *$|S|$ at the drain edge ($x = 26nm$ see Figure 1(b)) and* ***azimuth angle*** *θ (rotation in the x-y plane) as a function of* ***applied uniaxial strain*** *in the [001], [110] and [111] directions.*

We investigated the effects of strain by calculating the change in spin orbit coupling for applied strain in three crystallographic directions [001], [110] and [111] corresponding to a lattice difference of between 0 and 4% of the unstrained lattice, the results from this are plotted in Figure 6.

5. Conclusion and Outlook

We have demonstrated the successful inclusion of electron spin into a realistic model of a transistor.

Figure 4 shows that the average magnetisation starts off at a high value at the source which rapidly decays as the electrons pass through the channel, followed by a partial magnetization recovery due to spin refocusing as the electrons slow down to enter the drain.

From Figure 4(a) we see the magnetisation is sensitive to changes in gate voltages and to a lesser extent source-drain voltage this gives us a potential handle for control as the amount of magnetisation detected at the drain can be controlled by varying the gate voltage .

Mechanical strain also has large effect on the spin as increasing the strain changes the symmetries of both the lattice and quantum well increasing the amount of spin orbit coupling. This strain sensitivity has the potential to be used in a sensor whereby measuring the spin at the drain gives an indirect measure of the amount of molecular strain in the channel.

Future work is now under way to investigate spin-transport in different materials such as Si and the effects of low temperatures on the magnetisation decay and recovery.

References

[1] Thomas B. Bahder. Eight-band k. p model of strained zinc-blende crystals. *Physical Review B*, 41(17):11992, June 1990.

[2] Jaroslav Fabian, Alex Matos-Abiague, Christian Ertler, Peter Stano, and Igor Zutic. Semiconductor spintronics. *acta physica slovaca*, 54(4 & 5):565 – 907, August & October 2007.

[3] Aynul Islam, Brahim Benbakhti, and Karol Kalna. Monte carlo study of ultimate channel scaling in si and in 0.3 ga 0.7 as bulk mosfets. *IEEE Transactions on Nanotechnology*, 10(6):1424–1432, November 2011.

[4] Min Shen, Semion Saikin, Ming-C Cheng, and Vladimir Privman. Monte carlo modeling of spin fets controlled by spinorbit interaction. *Mathematics and Computers in Simulation*, 65:351–363, 2004.